Journal Pre-proof

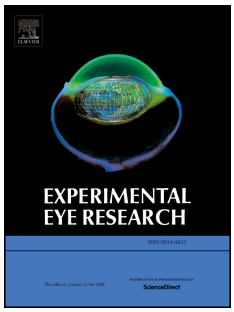

ON-bipolar cell gene expression during retinal degeneration: Implications for optogenetic visual restoration

Michael J. Gilhooley, Doron Hickey, Moritz Lindner, Teele Palumaa, Steven Hughes, Stuart N. Peirson, Robert E. MacLaren, Mark W. Hankins

PII: S0014-4835(21)00118-4

DOI: https://doi.org/10.1016/j.exer.2021.108553

Reference: YEXER 108553

To appear in: *Experimental Eye Research*

Received Date: 19 June 2020

Revised Date: 8 March 2021

Accepted Date: 23 March 2021

Please cite this article as: Gilhooley, M.J., Hickey, D., Lindner, M., Palumaa, T., Hughes, S., Peirson, S.N., MacLaren, R.E., Hankins, M.W., ON-bipolar cell gene expression during retinal degeneration: Implications for optogenetic visual restoration, *Experimental Eye Research* (2021), doi: https://doi.org/10.1016/j.exer.2021.108553.

Title Page

Title

ON-bipolar cell gene expression during retinal degeneration: implications for optogenetic visual restoration

Authors

Michael J Gilhooley[1,4,5,*]

Doron Hickey[1,3,*]

Moritz Lindner[1,4,6]

Teele Palumaa[2]

Steven Hughes[1,2]

Stuart N Peirson[2]

Robert E MacLaren[1,4,5]

Mark W Hankins [1,2,†]

Affiliations

1. Nuffield Laboratory of Ophthalmology, Nuffield Department of Clinical Neuroscience, University of Oxford, Oxford, United Kingdom OX1 3RE
2. Sleep and Circadian Neuroscience Institute, Nuffield Department of Clinical Neuroscience, University of Oxford, Oxford, United Kingdom OX1 3RE
3. Royal Victorian Eye and Ear Hospital, Melbourne, Australia 3002
4. The Oxford Eye Hospital, Oxford, United Kingdom OX3 9DU

5. Moorfields Eye Hospital, London, United Kingdom EC1V 2PD
6. Institute of Physiology and Pathophysiology, Department of Neurophysiology, Philipps University, Deutschhausstrasse 1-2, Marburg, Germany 35037

* The authors wish it to be known that, in their opinion, the first two authors should be regarded as joint first authors.

Corresponding Author

Contact Details

Email: mark.hankins@eye.ox.ac.uk

Telephone: +44 (0)1865 618 661

Funding

This work was supported by The Wellcome Trust (grant number 205151/Z/16/Z); The Wolf Fischer Trust; The German Research Foundation (DFG) (grant number LI2846/1-1) and The Biological Basic Sciences Research Council (grant number BB/M009998/1).

Conflict of Interest Statement

M.L.

Financial support – Heidelberg Engineering, Optos, Genentech, Alimera Sciences

Equity owner – Carl Zeiss Meditech, Fresenius Medical Care.

M.J.G., D.H., S.H., S.N.P., R.E.M. and M.W.H.

No relevant conflicts of interest

Statement

Aspects of this work were presented at the 2018 Association for Research in Vision and Ophthalmology annual meeting at Honolulu, Hawaii, USA.

Conclusion

Our findings suggest relatively few gene expression changes in the context of degeneration: that despite remodelling, bipolar cells are likely to remain viable targets for optogenetic vision restoration. In addition, several genes where changes were seen could provide a basis for investigations to enhance the efficacy of optogenetic therapies.

Keywords

Bipolar cell, gene expression, optogenetics, inherited retinal degeneration

Abbreviations

ANOVA – ANalysis Of VAriance

AAV – Adeno associated virus

EYFP – Enhanced Yellow Fluorescent Protein

FACS – Fluorescence Activated Cell Sorting

FDR – False detection rate

HSPG – Heparin Sulphate Proteoglycan

IHC – Immunohistochemistry

IRDs – Inherited Retinal Degenerations

P40, P90, P120, P150 – Postnatal day 40, 90, 120, 150

LTD/P – Long term depression / potentiation

PKC - Protein Kinase C -

qPCR – Quantitative Polymerase Chain Reaction

1. Introduction

Advances in retinal gene therapy delivery methods, such as adeno-associated virus (AAV), have allowed retinal gene replacement to become a reality for patients suffering from certain inherited retinal degenerations (IRDs)(Russell et al., 2017). With this success, attention has turned to expanding the use of these proven vectors with alternative strategies for visual restoration such as optogenetics - the expression of exogenous light sensitive proteins within an excitable cell - which may be applied to a wide range of IRDs, regardless of the causative mutation.

AAV delivered optogenetic tools have been shown to restore electrophysiological and behavioural responses to light in animal models of IRDs(Cehajic-Kapetanovic et al., 2015; De Silva et al., 2017; Doroudchi et al., 2011) by rendering surviving cells in the degenerate retina sensitive to light. This general principle of survivor cell stimulation has also been demonstrated clinically with electronic retinal prostheses already in clinical use for vision restoration(Edwards et al., 2018; Luo and da Cruz, 2016).

While effective, the stimulation of retinal ganglion cells - especially by epiretinal prostheses - bypasses much of the early image processing carried out in the retina. This makes specific stimulation of cells higher in the retinal hierarchy, such as the bipolar cell, conceptually attractive. However, significant retinal remodelling does occur after the death of the photoreceptor(Gilhooley and Acheson, 2017; Jones and Marc, 2005), potentially compromising the suitability of bipolar cells as targets for such stimulation. Indeed, changes in morphology, synaptic connections, electrophysiological responses and receptor expression(Dunn, 2015; Gayet-Primo and Puthussery, 2015; Kalloniatis et al., 2016; Marc and Jones, 2003; Marc et al., 2007; Marc et al., 2003; Varela et al., 2003) have been observed in human and animal studies.

To date, it is not understood how changes specifically within the bipolar cells during degeneration will affect their long-term viability as optogenetic targets. Particularly, if they are free from metabolic stress, receptive to adeno-associated viral vectors, suitable for opsin based optogenetic tools and able to propagate their signal by releasing neurotransmitter in response to exogenous optogenetic stimulation. While studies of general gene expression changes in animal models of the degenerate retina exist in the literature(Dorrell et al., 2004; Hackam et al., 2004; Hornan et al., 2007; Michalakis et al., 2013; Punzo and Cepko, 2007; Yu et al., 2018), none has considered the retinal bipolar cell in isolation.

Investigation of bipolar cells is particularly apposite for two reasons: first, the development of delivery tools to specifically target discrete retinal cell populations (such as cell specific promoters and AAV capsid tropism(Cronin et al., 2014; de Leeuw et al., 2014; de Silva et al., 2015; Juttner et al., 2019; Kleine Holthaus et al., 2020; Lu et al., 2016; Scalabrino et al., 2015)) have made cell-specific delivery a realistic possibility. Secondly, human opsins such as rhodopsin(Cehajic-Kapetanovic et al., 2015; Gaub et al., 2015), cone opsin(Berry et al., 2019), melanopsin(De Silva et al., 2017; Lin et al., 2008) and variants(van Wyk et al., 2015) are being described as sensitive optogenetic tools. These are known to couple to endogenous G-protein signalling cascades(Hughes et al., 2016) allowing greater signal amplification compared to microbial opsins, such as channelrhodopsin(Lagali et al., 2008), which lack such coupling. However, this coupling could be affected by changes in levels of constituents of these cascades in bipolar cells during retinal degeneration. Therefore, investigation of retinal bipolar cells specifically in IRD models is paramount in determining if this conceptually attractive strategy of bipolar specific targeting is likely to be feasible for the clinical translation of optogenetics.

The principal objective of this study was to confirm the continued expression of the principal components of both the ON-bipolar light signalling and other second messenger cascades during IRDs. Here we show that, despite remodelling, bipolar cells undergo remarkably limited transcriptomic changes in response to the loss of synaptic inputs from photoreceptors, even in the late stages of the disease in an animal model.

The secondary aim of the study was to identify differentially expressed genes for further characterisation in both *Pde6b*$^{wt/wt}$ and *Pde6b*$^{rd1/rd1}$ retinae using immunohistochemistry. Together, these findings will be central to guiding investigations to effectively translate bipolar cell targeted optogenetic therapies into clinical use.

2. Methods

2.1 Mouse lines

All experiments involving animals were performed in accordance with the Animals for Scientific Procedures Act 1986, licence no. 30/3371 and approved by the University of Oxford animal welfare and ethical review body and in accordance with the declaration of Helsinki and the ARVO Statement for the Use of Animals in Ophthalmic and Vision Research. A transgenic mouse line ("L7.Cre.EYFP.Pde6b$^{x/x}$", supplementary methods) was used which:

1. Expressed Cre recombinase under the control of the ON-bipolar cell specific promoter "L7" (also known in the literature as "Pcp2"),
2. Were homozygous for "floxed" EYFP at the Rosa26 locus and therefore expressed EYFP in L7 (retinal ON-bipolar) cells.
3. Were either Pde6b$^{wt/wt}$ or Pde6b$^{rd1/rd1}$ (wildtype or retinal degeneration phenotype)

2.2 Isolation of RNA from retinal bipolar cells and comparison with gene array

Six L7.Cre.EYFP.Pde6b$^{wt/wt}$ and Six L7.Cre.EYFP.Pde6b$^{rd1/rd1}$ mice underwent cervical dislocation at P89 to P91, six hours into their light phase with immediate enucleation. All mice were littermates, three of each group were female. Retinae were dissected with special care to remove retinal pigment epithelium before cell dissociation using a papain dissociation kit (Worthington Biochemical, Lakewood, USA) according to the manufacturer's instructions (figure 1).

The resulting dissociated cells were subjected to fluorescent activated cell sorting (FACS) (figure 1) with 97.3±1.8% of cells in the YFP+ isolate co-staining for PKC on ICC. RNA was extracted from cell isolates and processed using standard methods for use on a MouseWG-6 v2 Expression BeadChip (Illumina). Expression levels were compared using

Lumi(Du et al., 2008) and Limma(Ritchie et al., 2015) packages for R(Team, 2013) with quintile normalization. Results were corrected for multiple testing using FDR testing(Benjamini, 1995) (*supplementary methods*).

When isolating dissociated retinal cells in such a way, the large number of rod photoreceptor cells in the wildtype retina as well as their invaginated bipolar cell synapses could potentially lead to rods being carried over with labelled bipolar cells into the isolate. Increasing the length of enzymatic dissociation can minimise rod contamination, yet such approaches must be weighed against the risk of damage to the isolated cells or RNA with extended papain dissociation times. These protocols not only require longer periods for cells in a 'non-physiological' state before mRNA extraction, but lead to greater loss of cell processes (dendrites and axons). These are especially relevant to bipolar cells given the dramatic changes to these parts of the cell during degeneration.

Previous studies have attempted to control for rod carry over in different ways - for example, Siegert et al(Siegert et al., 2012) normalise all gene expression levels based on expression of known rod specific genes whereas Punzo et al(Punzo and Cepko, 2007), exclude any known rod specific genes from further analysis while Berg et al(Berg et al., 2019) examine changes in array expression of known photoreceptor genes to quantify levels of contamination.

We specifically interrogated our samples (prior to gene array) for two known rod specific genes (*Rho & Cnga1*) in a small number of samples using qPCR to confirm relative sample purity (*supplementary methods, Figure 1*). Despite this, our gene array data did present differential expression of a small number of genes with either a rod ontological annotation or where previous literature reported low or absent protein expression in bipolar cells compared to photoreceptors (*table S1*). To avoid difficulties in interpretation,

we excluded these genes from further investigation(Berg et al., 2019; Punzo and Cepko, 2007) but did not systematically alter our data otherwise(Siegert et al., 2012). Like all of the approaches described above, this relies on an (fortunately available) *a priori* knowledge of gene photoreceptor specificity which should be borne in mind when extrapolating conclusions beyond this model.

2.3 Identifying candidate genes for further investigation

As in previous studies, we combined several practical strategies to prioritise those probes found to have significantly different expression for further investigation(Berg et al., 2019; Michalakis et al., 2013; Punzo and Cepko, 2007; Siegert et al., 2012). After removal of genes with rod annotations (*table S1*) interaction & pathway prediction software(Fabregat et al., 2016; Warde-Farley et al., 2010) was used to identify shared functions or pathways linking groups of differentially expressed genes. All differentially expressed genes were also searched for on the *RetNet(Daiger et al., 1998)* database of human retinal disease genotype-phenotype relations to identify potentially clinically relevant candidates.

For each candidate, a search was performed on the NCBI® Gene database to extract gene ontology annotations and on the Medline® database allow systematic review of the literature (*supplementary methods*). Gene ontology terms were used to group the genes into six broad functional groups (*table 1*) while review of primary literature allowed prioritisation of an initial candidate in each group for further investigation (*supplementary methods*) and identification of any potential photoreceptor specific genes (*table S1*). Within each of first four groups, one candidate was prioritised (*supplementary methods*) to be further characterised by IHC staining.

2.4 Immunohistochemistry & semiquantitative image analysis

At each of four timepoints (P30, P90, P120 and >P150), *Pde6b*$^{wt/wt}$ and *Pde6b*$^{rd1/rd1}$ mice (n=3 per genotype, unless otherwise indicated) underwent cervical dislocation before immediate

enucleation and processing of retinae for IHC (*supplementary methods*). Images were taken at a point three fields of view (at x40 magnification) from the ora serata in three sections from one eye in each animal. Colocalised staining for the proteins of interest and a bipolar cell marker were taken as a semiquantitative index of protein expression levels in bipolar cells and were determined using Costes' method, described and validated previously (Costes et al., 2004). In brief, this involves normalising the number of pixels demonstrating colocalization above threshold in each image to the number of non-zero pixels in the image to give an index of colocalization that could be compared between images (*supplementary methods*). A two-way ANOVA with Sidak's method to account for multiple comparisons between groups and Tukey's test for comparison with groups over time.

3. Results

3.1 Gene Array Comparison

Retinal ON-bipolar cells were isolated using FACS of dissociated retina from L7.Cre.EYFP transgenic mice which were additionally either wildtype or homozygous for a clinically relevant IRD mutation (Pde6b$^{wt/wt}$ or Pde6b$^{rd1/rd1}$). cDNA libraries were extracted from the resulting EYFP+ (ON-bipolar) cell isolates were processed and subjected to an Illumina® mouse gene array. To quantify contamination of these isolates with rod photoreceptors, qPCR for two rod specific genes (Cnga1, Rho, chosen a priori) was performed to ensure that neither was detectable at a significant level in any bipolar cell isolate (Cnga1 – undetectable, Rho <1% in YFP + isolate compared to YFP -, Supplementary methods). Gene array analysis revealed sixty-six probes corresponding to sixty genes were shown to have differential expression between the degenerate and non-degenerate samples with a p value of <0.05 (False detection rate (FDR) testing, figure 1, tables 1 & S2, supplementary methods).

3.2 Candidate Genes

Following this, a sequence of methods was employed to highlight the most relevant genes, beginning with pathway analysis and database searches to highlight groups of genes with common function. Protein-protein interaction prediction software(Warde-Farley et al., 2010) highlighted one common function ("transition metal ion binding") linking five of the differentially expressed genes (Atox1, Clip1, Msrb2, Mt1 & Mt2) involved in preventing and repairing oxidative damage. This was reinforced by use of the Reactome® knowledge base(Fabregat et al., 2016), demonstrating two similar overrepresented pathways ("Metallothionein metal binding" p=0.009 & "Response to metal ions" p=0.013) involving similar genes (Msrb2, Mt1 & Mt2). Searches of the RetNet database(Daiger et al., 1998) revealed only one differentially expressed gene (Srm2) to be implicated in human retinal disease.

Genes known to be related to the native bipolar cell light signalling pathway (*Grm6 +1.054, p=0.8573; Gnao1 -1.23, p=0.9835; Gnb5 -1.13, p=0.9670; Gng13 -1.01, p=0.7109; Trpm1 +1.19, p=0.8035 (log_2 fold change, adjusted p value, FDR, table S3, figure S3)* were specifically queried, and while highly expressed in absolute terms, none were significantly differentially expressed between groups. Similarly queried were genes more generally implicated in cell signalling (*table S3*) and remodelling (*e.g. glutamate, glycine and GABA receptors, table S4*) with no significantly differentially expressed genes identified.

As these methods revealed only one unifying functional pathway - "metal ion binding" (*supplementary results*) – this data driven approach was complemented by a manual, systematic, evaluation (including literature and gene ontology consortium annotation review) for each differentially expressed gene. This was used to group the potential candidates by function(Harris et al., 2004) and score them for relevance to our research question (*supplementary methods*). The highest scoring potential candidate in each group was selected for further investigation at the protein level using IHC: Srm2, coding for a gene involved in cell shape regulation, *Slf2* heparin proteoglycan metabolism, *Anxa7*, neurotransmitter release and *Cntn1* in synaptic remodelling *(see Table1)*.

3.3 Immunohistochemical staining

Antibody labelling for proteins encoded by each of the selected genes (*Srm2, Sulf2, Anxa7, Cntn1)* showed co-localisation with classical ON bipolar markers (CHX10 or PKCa) at postnatal day 90 (P90) in our IHC study – although these proteins were typically *not* expressed exclusively within ON BCs (*figures 2-5*). A semi-quantitative index of staining was recorded for each genotype (*Pde6b$^{wt/wt}$ & Pde6b$^{rd1/rd1}$*) at each timepoint (P40, P90, P120, P150) to give an impression of how protein levels may change over time.

There was a difference between genotypes in this index for all proteins excepting *slf2* (Sulphatase 2) [*Srm2* F(1, 8) = 23.85; *p*=0.0012, *Slf2* F(1, 8) = 3.775 ; *p*=0.0879, *Anxa7* F(1, 9) = 5.31; *p*=0.0467; *Cntn1* F(1, 13) = 8.272; *p*=0.0130]. In addition, differences in staining over time were seen in *Srm2* (Shroom 2) & *Slf2* [*Srm2* F(3, 8) = 4.865; *p*=0.0327, *Slf2* F(3,8) = 19.9; *p*=0.005, *Anxa7* F(3, 9) = 0.1829; *p*=0.9053, *Cntn1* F(3, 13) = 0.168; *p*=0.9161]. Whilst an interaction between genotype and time was seen in *Srm2* and *Cntn1* (Contactin 1) [*Srm2* F(3,8) = 0.09; *p*=0.0059, *Slf2* F(3,8) = 2.718; *p*=0.1148, *Anxa7* F(3,9) = 0.6712; *p*=0.5909, *Cntn1* F(3,13) = 7.366; *p*=0.0039]. (*Please see Figures 2-5 and supplementary material for post hoc analysis*)

Discussion

4.1 Bipolar cells

Much of mammalian basic image processing is initiated within the neural retina before signals reach retinorecipient visual centres. As vision is lost in the IRDs through preferential photoreceptor (PR) death, the retinal bipolar cells become the highest surviving cells of this neural hierarchy. As such, their stimulation may - in principle - enable more intra-retinal processing to be preserved at the synapses of the inner plexiform layer, presenting them as particularly attractive targets for optogenetic visual restoration.

Targeting bipolar cells assumes that, within a degenerate retina, these cells retain levels of the second messengers required for light signalling. It also assumes such cells survive in a stable state without metabolic stress to allow effective propagation of this signal by synaptic neurotransmitter release and, importantly, are able to be transduced by AAV. Increasing evidence confirms that bipolar cells do undergo significant remodelling in the later stages of retinal degeneration with changes in morphology, synaptic connections, electrophysiological responses and receptor expression (Cuenca et al., 2014; Dunn, 2015; Gayet-Primo and Puthussery, 2015; Kalloniatis et al., 2016; Marc and Jones, 2003; Marc et al., 2007; Michalakis et al., 2013; Strettoi et al., 2002).

4.2 Gene expression in context

Here we show that, despite this remodelling, bipolar cells undergo remarkably limited transcriptomic changes in response to the loss of synaptic inputs from photoreceptors, even in the late stages of the disease. While gene array studies of whole retina may not have statistical power to detect very small changes in expression of single genes, our approach of limiting our comparison as far as possible to a single cell type in a clinically relevant disease model, will accentuate those changes that are biologically most relevant.

Given the marked changes seen at the anatomical level over the whole retina during the neural remodelling of degeneration, it is perhaps surprising that we found such a small number of genes were differentially expressed in bipolar cells in this context (66 out of a total of c.20,000 probes). The absence of differential expression of genes related to the native bipolar cell light signalling cascade, second messaging in general or glutaminergic transmission (*tables S3 & S4)* is particularly interesting given reports of functional loss of sensitivity to glutamate even early in degeneration (Varela et al., 2003). We see no significant alteration in expression of genes associated with glutamate receptor subunits (nor with GABAergic, nor glycinergic receptors, *table S4*) which is intriguing given the shift from metabotropic to ionotropic transmission seen at a functional and anatomic level in bipolar cells during degeneration (Dunn, 2015; Marc et al., 2007; Varela et al., 2003).

This finding of such stability at a gene expression level is particularly informative when seen in the light of studies where opsin based optogenetic tools (Cehajic-Kapetanovic et al., 2015; De Silva et al., 2017; Lin et al., 2008) are targeted to ON-bipolar cells to functionally restore light responses in degenerate retina. Therefore, despite marked functional and anatomical remodelling, the parts of the bipolar cell signalling cascade necessary for optogenetic restoration appear to persist both at a gene expression and functional level during retinal degeneration in the *Pde6b*^{rd1} model. Given that the *rd1* mutation causes an IRD in humans similar in phenotype to that of the model, these findings are particularly interesting from a translational point of view (if they are reflected in human bipolar cells). In counterpoise however, the huge variety of causative mutations in human IRDs should still be borne in mind when extrapolating results.

4.3 Identifying Candidate Genes

With a relatively small number of differentially expressed genes overall and no obvious candidate genes presented for further investigation by data driven approaches *(supplementary results)*, a systematic literature review for each gene could be used to group and prioritise those most promising for further characterisation at the protein level (*Srm2, Slf2, Anxa7, Cntn1*). Immunohistochemical staining at the timepoint corresponding to the gene array (P90) confirmed expression of all four proteins in bipolar cells of both *Pde6b*$^{wt/wt}$ and *Pde6b*$^{rd1/rd1}$ retinae. Staining of similar retinae at other timepoints over the course of degeneration (*figures 2 to 5, table 2*) could be additionally analysed in a semi-quantitative manner to given an impression of likely relative protein expression over time in order to guide potential future investigations.

4.4 Further characterisation of selected candidate genes

The pattern of Shroom 2 staining (*figure 2*) that we see in degeneration, with a maxima in mid degeneration (where neural modelling is at its highest), is consistent with its described role in cytoskeleton remodelling, cell shape regulation and membrane blebbing, given the retraction of bipolar cells axons and change in shape seen in histological studies of degeneration (Jones and Marc, 2005; Strettoi et al., 2002). A corresponding upturn in staining at P150 in wildtype animals was seen in multiple replicates and could perhaps be explained by an increase in neural remodelling in older mice – which would certainly be an interesting target for further investigation. In the broadest terms, this may suggest intervention earlier in the course of degeneration may be beneficial whilst cytoskeleton and membrane activity (such as AAV entry, payload trafficking and neurotransmitter release) are possibly less disrupted.

The Heparin Sulphate Proteoglycans (HSPG), from which Sulphatase 2 removes sulphate residues, are involved in (but not essential to) the binding of AAV in advance of its entry to the cell (Summerford and Samulski, 1998). Importantly, AAVs are less able to bind HSPGs that are less sulphonated (for example due to increased sulphatase activity) and indeed HSPGs have been found to be functionally important in retinal cell transduction efficiency, especially by the intravitreal route (Boye et al., 2016; Woodard et al., 2016). Interestingly, our semiquantitative IHC (*figure 3*), unlike gene array data, suggests no difference in Sulphatase 2 staining compared to wildtype during degeneration. However, this could represent an increase in protein turnover (and hence RNA levels), a shift to the secreted, extracellular form of the protein during degeneration(Morimoto-Tomita et al., 2002) from the cell surface bound sulphatase 2 or indeed post-transcriptional changes at the mRNA level and so gene expression levels do not directly reflect the level of cell staining. Therefore, it may be fruitful to investigate quantitatively HSPG sulphonation in various cell types of the degenerate retina, compared to wildtype. Or indeed, if changes in *Sulf2* levels can manipulate AAV transduction efficiency (for example by investigating AAV transduction in a *Sulf2* knock out retinae (table 2).

Effective retinal optogenetic therapy requires neurotransmitter release from targeted cells; Annexin a7 is central to this process and interacts with PKCα, an enzyme known to regulate bipolar cells' light response kinetics (*table 2*) (Hoque et al., 2014) *(supplementary discussion)*. *Anxa7* IHC staining in our series is just significantly different from wildtype during degeneration (but with no individual timepoint identified as significant on post hoc analysis), this could suggest that this aspect of the bipolar signalling cascade is indeed still functional, but with a reduced rate of protein turn over when light signalling is lost during retinal degeneration. A more comprehensive understanding of the role of *Anax7*'s in the

wildtype bipolar cell light response will need to be determined if any downregulation is likely to directly impair bipolar cells ability to act as optogenetic targets, or indeed represent an opportunity to manipulate response kinetics.

To act as optogenetic targets, bipolar cells must not only be able to release neurotransmitter, but to maintain useful synapses to communicate the transduced light signal. Contactin 1 has a role in regulating synaptic plasticity in the nervous system, so our finding that it was *downregulated* at P90 in retinal degeneration – a process defined by neural remodelling (Jones and Marc, 2005) - was perhaps surprising. The transient drop in IHC staining (at P90 only) in our series (*figure 5 and table 2*) is however congruent with the findings of Haenisch et al who also noted an initial marked decrease of neural *Cntn1* mRNA expression followed by an increase back to baseline when investigating nerve crush (deafferention) in zebra fish (Haenisch et al., 2005). Which, in isolation, could perhaps predict a benefit to early optogenetic intervention in the retina, restoring afferent signal input in an attempt to prevent a drop in Contactin 1 and any resulting maladaptive synaptic remodelling.

4.5 Limitations

While representing the first description of transcriptomic changes in bipolar cells in the context of degenerative retina remodelling, there are limitations to our approach that must be borne in mind when extrapolating results.

Firstly, as alluded to above, we predicted that rod photoreceptors may be a contaminant of our cell isolates and therefore assessed sample purity in two ways – by interrogating our microarray samples for expression of genes known to be specific for rods and by performing RT-qPCR for a small number of these markers. However we did not quantify markers specific to other retinal cell types to absolutely exclude contamination from other populations.

Secondly, microarrays incorporate multiple technical controls and have been shown to faithfully replicate the mRNA quantification results of other methods (such as qPCR) (Arikawa et al., 2008; Canales et al., 2006; Morey et al., 2006) and in meta-analysis studies show concordance across array platforms(Brown et al., 2017). Therefore, we did not employ alternative methods to externally validate our microarray findings at the mRNA level, but rather, investigated a subset of candidate genes by IHC. This approach provided a wealth of additional information on both the spatial distribution within the retina as well as whether mRNA changes actually affected protein levels. However, mRNA modifications, transport and post translational modifications could potentially occur. Indeed, further investigation of such processes will form an important future direction of investigation – especially as they may explain the lack of change in staining for Sulf2 & Anxa7 at P90.

Thirdly, as this is the first study to investigate transcriptional changes in on-bipolar cells during retinal degeneration, a direct positive-control - a gene already known to be up or down regulated in this context – was lacking. Such positive controls provide a valuable technical validation of transcriptomic datasets but were not possible in this context.

5. Conclusion

Here we present the first comparison of gene expression in bipolar cells of degenerate and non-degenerate retinae. Our findings suggest relatively few changes in gene expression with degeneration, including genes essential to effective optogenetic bipolar light signalling. This suggests, that despite remodelling, bipolar cells are likely to remain viable and effective targets for optogenetic vision restoration and we highlight candidate genes where further investigation is likely to improve the translation of this important technique.

Acknowledgements

George Nicholson for assistance in producing figure S1.

Cambridge Genomic Services for performing the Illumina gene microarray.

Figure and Table Legends

Figure 1.

1.1 Experimental Approach: fluorescence-activated cell sorting for a microarray study of retinal bipolar cells from degenerate retinas. (A)L7-Cre EYFP non-degenerate ($Pde6b^{wt/wt}$) and degenerate ($Pde6b^{rd1/rd1}$) mice were culled at P90 and the retinae removed with careful dissection to remove Retinal Pigment Epithelium before dissociation (B) FACS was then used to isolate YFP-positive (ON-Bipolar) cells (C). From this isolate, RNA was extracted (D) and used for a microarray study. Panel (C1) represents an illustrative FACS dot plot of a single dissociated, non-degenerate L7.Cre.EYFP retinae and (C3) the same from a degenerate retina.

1.2 FACS Validation. Methods to confirm the identity of isolated YFP+ cells. (A) Immunocytochemistry (ICC) of YFP positive and YFP negative FACS isolate stained for DAPI (blue), PKCa (red) and YFP (green) showing, as expected enrichment of PKC + (bipolar) cells in the YFP+ isolate. Scale bars = 50µm. (B) Quantitative PCR (qPCR) comparing expression of retinal bipolar cell-specific and rod cell-specific genes in the YFP-positive cell population, relative to the YFP- negative cell population in samples from a small number of wildtype and degenerate ($Pde6b^{rd1/rd1}$) L7-Cre EYFP retinas following FACS at P90. The YFP-positive cell fraction had higher expression of bipolar-specific and lower expression of rod-specific genes, indicating that the YFP-positive population was enriched in bipolar cells (mean ± s.e.m.; n = 2, non- degenerate, n = 1, degenerate).

Table 1. Genes differentially expressed between *Pde6b*$^{rd1/rd1}$ and *Pde6b*$^{+/+}$ retinae at P90, grouped by broad function based on gene ontology terms annotated to the gene's entry on the gene ontology consortium database (two listed for each gene). □ = change in expression compared to *Pde6b*$^{wt/wt}$ (i.e. '+' = up regulated; '-' = down regulated) please see table S2 for corresponding FDR adjusted p-values.

Table 2 Details of four differentially expressed genes prioritised for further characterisation with IHC. The bottom four rows refer to semiquantitative IHC co-localisation seen in figure 2,3,4 and 5. *p*= - "adjusted p value"; n.s. – P>0.05

Figure 2. Shroom 2 Immunohistochemistry (upregulated on gene array at P90)

(A) Retinal cross sections from Pde6b$^{rd1/rd1}$ and Pde6b$^{wt/wt}$ mice stained for DAPI (blue), CHX10 (green) and Shroom2 (red). ONL – Outer nuclear layer, OPL – Outer Plexiform layer, INL- Inner nuclear layer, IPL –inner plexiform layer, GCL – Ganglion cell layer. Scale bar = 20µm. White box indicates area from which close up images in panels B & D are taken.

(B&D) Close up images of bipolar cell bodies in *Pde6b*$^{rd1/rd1}$ retina (B) and *Pde6b*$^{wt/wt}$ (D) at four time points during degeneration (P40, P90, P120, P150). CHX10 (green) and shroom 2 (red). Scale bars = 5µm

(C) Colocalised pixels above threshold - a semiquantitative index of protein staining. Normalised to highest value over all retinae stained for shroom 2. Dots represent the mean value for each animal, lines connect the means for each group at that timepoint. Star markers on graph represent adjusted p values, Sidak's method for multiple comparison (see results section for details): P90 p=0.0136; P120 p=0.0026 red line = *Pde6b*$^{rd1/rd1}$; blue line = *Pde6b*$^{wt/wt}$.

Figure 3. Sulphatase 2 Immunohistochemistry (upregulated on gene array at P90)

(A) Retinal cross sections from Pde6b$^{rd1/rd1}$ and Pde6b$^{wt/wt}$ mice stained for DAPI (blue), PKC□ (green) and sulphtase 2 (red). ONL – Outer nuclear layer, OPL – Outer Plexiform layer, INL- Inner nuclear layer, IPL –inner plexiform layer, GCL – Ganglion cell layer. N.B. Due to primary antibodies being raised in differing species, to allow co-staining of sections, PKC□ is used as an ON-bipolar marker here, rather than CHX10. Scale bar = 20µm. White box indicates area from which close up images in panels B & D are taken.

(B&D) Close up images of bipolar cell bodies in *Pde6b*$^{rd1/rd1}$ retina (B) and *Pde6b*$^{wt/wt}$ (D) at four time points during degeneration (P40, P90, P120, P150). PKC□ (green) and Sulphatase 2 (red). Scale bars = 5µm

(C) Colocalised pixels above threshold - a semiquantitative index of protein staining. Normalised to highest value over all retinae stained for Sulphatase 2. Dots represent the mean value for each animal, lines connect the means for each group at that timepoint. Star markers on graph represent adjusted p values, Sidak's method for multiple comparison (i.e.

None reaching significance, see results section for details). red line = *Pde6b*$^{rd1/rd1}$; blue line = *Pde6b*$^{wt/wt}$

Figure 4. Annexin a7 Immunohistochemistry (downregulated on gene array at P90).

(A) Retinal cross sections from Pde6b$^{rd1/rd1}$ and Pde6b$^{wt/wt}$ mice stained for DAPI (blue), CHX10 (green) and annexin a7 (red). ONL – Outer nuclear layer, OPL – Outer Plexiform layer, INL- Inner nuclear layer, IPL –inner plexiform layer, GCL – Ganglion cell layer. Scale bar = 20µm. White box indicates area from which close up images in panels B & D are taken.

(B&D) Close up images of bipolar cell bodies in *Pde6b*$^{rd1/rd1}$ retinae (B) and *Pde6b*$^{wt/wt}$ (D) at four time points during degeneration (P40, P90, P120, P150). CHX10 (green) and annexin a7 (red). Scale bars = 5µm.

(C) Colocalised pixels above threshold - a semiquantitative index of protein staining. Normalised to highest value over all retinae stained for annexin a7. Dots represent the mean value for each animal, lines connect the means for each group at that timepoint. Star markers on graph represent adjusted p values, Sidak's method for multiple comparison (i.e. None reaching significance, see results section for details). red line = *Pde6b*$^{rd1/rd1}$; blue line = *Pde6b*$^{wt/wt}$

Figure 5. Contactin1 Immunohistochemistry (downregulated on gene array at P90).

(A) Retinal cross sections from Pde6b$^{rd1/rd1}$ and Pde6b$^{wt/wt}$ stained for DAPI (blue), CHX10 (green) and Contactin 1 (red). ONL – Outer nuclear layer, OPL – Outer Plexiform layer, INL- Inner nuclear layer, IPL – inner plexiform layer, GCL – Ganglion cell layer. Scale bar = 20µm. White box indicates area from which close up images in panels B & D are taken.

(B&D) Close up images of bipolar cell bodies in *Pde6b$^{rd1/rd1}$* retina (B) and *Pde6b$^{wt/wt}$* (D) at four time points during degeneration (P40, P90, P120, P150). CHX10 (green) and Contactin 1 (red). Scale bars = 5µm.

(C) Colocalised pixels above threshold - a semiquantitative index of protein staining. Normalised to highest value over all retinae stained for Contactin 1. Dots represent the mean value for each animal, lines connect the means for each group at that timepoint. Star markers on graph represent adjusted p values, Sidak's method for multiple comparison at P90 p=0.0026) (see results section for details). red line = Pde6b$^{rd1/rd1}$; blue line = *Pde6b$^{wt/wt}$*

Symbol	Δ $\log_2$	Ontology term 1	Ontology term 2
A - Actin cytoskeleton, microtubules and intracellular transport			
Ap3m2	-1.85	anterograde synaptic vesicle transport	intracellular protein transport
Cng	3.52	microtubule cytoskeleton organization	microtubule binding
Sept4	1.54	cilium assembly	mitotic cytokinesis
Srm2	**1.81**	**actin cytoskeleton organization**	**melanosome organization**
Tmsb10	-2.15	actin cytoskeleton organization	regulation of cell migration
B - Heparin sulphate proteoglycan metabolism			
Extl3	-2.05	heparan sulphate proteoglycan biosynthesis	protein glycosylation
Sulf2	**1.43**	**heparan sulphate proteoglycan metabolic process**	**arylsulfatase activity**
C - Cell signalling, calcium homeostasis			
Anxa7	**-1.56**	**calcium ion binding**	**membrane fusion**
Cabyr	2.25	sperm capacitation	calcium-mediated signalling
Gabrg2	-1.56	gamma-aminobutyric acid signalling pathway	synaptic transmission, GABAergic
Pde1c	-1.96	signal transduction	response to calcium ion
Slc7a3	-2.87	amino acid transport	arginine transport
Unc13a	-2.11	neurotransmitter secretion	SNARE binding
D - Neural cell growth, survival & remodeling			
Cntn1	**-1.79**	**neuron projection development**	**nervous system development**
Efnb1	2.15	axon guidance	presynapse assembly
Hdac9	-3.69	DNA repair	chromatin organization
Lynx1	-8.26	synaptic transmission, cholinergic	acetylcholine receptor binding
Mif	-1.91	regulation of cell proliferation	positive regulation of axon regeneration
Nrm	-1.40	nuclear membrane	membrane
Pcdha7	-1.98	cell adhesion	cell-cell recognition
Phc1	1.93	cellular response to retinoic acid	histone ubiquitination
Ptprr	-3.72	negative regulation of ERK1 and ERK2 cascade	ERBB2 signalling pathway
Sfrs1	1.72	mRNA 5'-splice site recognition	regulation of transcription, DNA-templated
Socs5	-1.64	regulation of growth	JAK-STAT cascade
Yaf2	-2.54	regulation of transcription, DNA-templated	transcription, DNA-templated
E - Aerobic and anaerobic respiration, cellular response to stress			
Atox1	-1.62	transition metal ion binding	response to oxidative stress
Clip1	-2.75	transition metal ion binding	microtubule bundle formation
Cox3	-1.83	aerobic electron transport chain	aerobic respiration
Msrb2	3.03	transition metal ion binding	cellular response to stress
Mt1	-10.73	transition metal ion binding	cellular metal ion homeostasis
Ndufb2	-1.55	mitochondrial respiratory chain complex I	oxidation-reduction process
Pgk1	-2.30	glycolytic process	carbohydrate metabolic process
F - Miscellaneous			
Abca1	-3.10	cholesterol homeostasis	cellular response to retinoic acid
Fam19a3	1.87	positive regulation of microglial cell activation	negative regulation of microglial cell activation
Naa11	-3.83	n-terminal protein amino acid acetylation	n-terminal peptidyl-glutamic acid acetylation
Rnf11	-1.75	protein autoubiquitination	ubiquitin-dependent protein catabolic process

MJ Gilhooley, D Hickey, M Lindner, T Palumaa, S Hughes, S Peirson, RE MacLaren, MW Hankins

"Retinal bipolar cell gene expression during retinal degeneration: implications for optogenetic visual restoration"

Supplementary Figures & Tables

February 2021

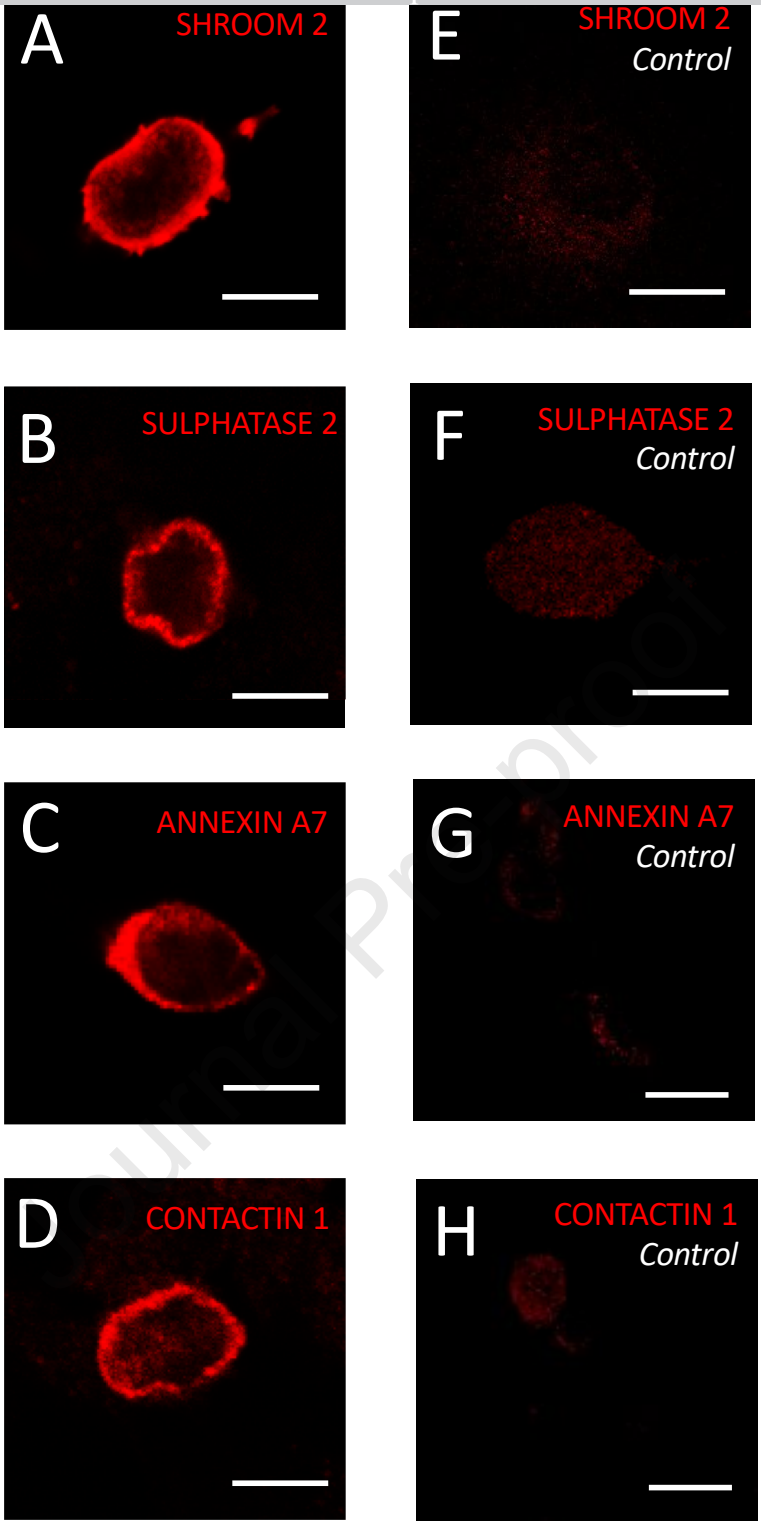
A
SHROOM 2
E
SHROOM 2
Control
B
SULPHATASE 2
F
SULPHATASE 2
Control
C
ANNEXIN A7
G
ANNEXIN A7
Control
D
CONTACTIN 1
H
CONTACTIN 1
Control

(Fig S1.)

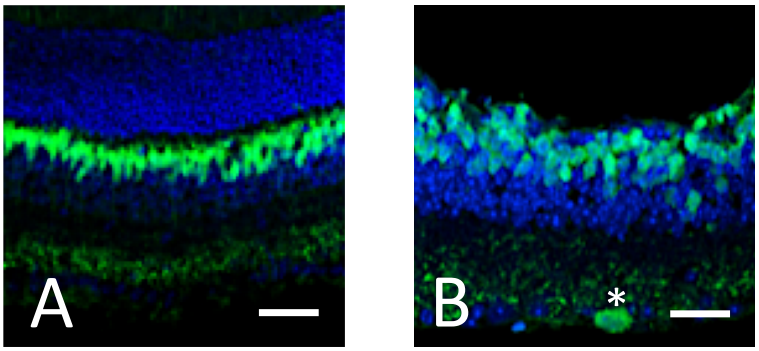
A
B
*

(Fig S2.)

Figure S1. Validation of antibodies. ICC images of HEK293T cells transfected to express the protein corresponding to the labelled antibody. As can be seen, all four stain at a level far above that of a non-transfected control. Note staining pattern of all four antibodies is consistent with protein in or around the cell membrane.
A – D Appropriately transfected HEK293T cells stained with the respective antibody
E – H Untransfected HEK293T cells stained with the respective antibody
Scale bars - 10μm

Figure S2. L7.Cre.EYFP mice express EYFP in rod and cone type 2 & 6 bipolar cells as well as a small subset of bistratified retinal ganglion cells (circa 1,500 in retina, denoted by asterix). Blue = DAPI, Green = YFP Scale bars = 15μm

(A) On a *Pde6b*$^{wt/wt}$ background
(B) On a *Pde6b*$^{rd1/rd1}$ background

Probe/gene name	log_2 fold change	p value
Rod Specific		
Gnat1	-21.14	0.0002
Pdc	-1.83	0.0421
Pde6b	-3.47	0.0004
Nrl	-2.79	0.0380
Sag	-6.01	0.0009
Slc24a1	-5.27	0.0231
Pde6g	-3.02	0.0473
Reep6	-2.56	0.0380
Esrrb	-2.00	0.0153

Probe/gene name	log_2 fold change	p value
Rod contentious		
Gpnmb	-4.14	0.0035
Ldha	-4.61	0.0014
Car2	-2.94	0.0004
Adcy1	-2.97	0.0004

Table S1. (A) Genes with rod specific ontological annotation; (B) Genes with literature suggesting contentiousness due to low bipolar compared to photoreceptor protein expression. A positive log fold change represents upregulation in degenerate samples. *"p* value" represents the adjusted p-value following False Detection Rate (FDR) testing.

Symbol	Probe/gene name	log_2 fold Δ	p value
A - Probes upregulated in degeneration			
Igfn1	Immunoglobulin-like and fibronectin type III domain containing 1	4.10	0.0181
Cgn	Cingulin	3.52	0.0138
Msrb2	Methionine sulfoxide reductase B2	3.03	0.0344
Cabyr	Calcium binding tyrosine-(Y)-phosporylation regulated	2.25	0.0380
Efnb1	Ephrin-B1	2.15	0.0312
Ccdc171	Coiled-coil domain containing 171	1.99	0.0458
Phc1	Polyhomeotic homolog 1	1.93	0.0276
Sfxn1	Sideroflexin 1	1.92	0.0195
Fam19a3	Family with sequence similarity 19 (chemokine (C-C motif)-like) A3	1.87	0.0458
Shroom2	Shroom family member 2	1.81	0.0416
Sfrs1	Serine/arginine-rich splicing factor 1	1.72	0.0417
Sept4	Septin 4	1.54	0.0324
Sulf2	Sulfatase 2	1.43	0.0344
B - Probes downregulated in degeneration			
Nrm	Nurim (nuclear envelope membrane protein)	-1.40	0.0416
Gm362	Predicted gene 362	-1.46	0.0138
Pde9a	Phosphodiesterase 9A	-1.55	0.0416
Ndufb2	NADH dehydrogenase (ubiquinone) 1 beta subcomplex, 2	-1.55	0.0414
Gabrg2	Gamma-aminobutyric acid (GABA) A receptor, gamma 2	-1.56	0.0494
Anxa7	Annexin A7	-1.56	0.0244
Fam195a	Family with sequence similarity 195, member A	-1.61	0.0053
Atox1	Antioxidant 1 copper chaperone	-1.62	0.0414
Socs5	Suppressor of cytokine signaling 5	-1.64	0.0149
Csrnp2	Cysteine-serine-rich nuclear protein 2	-1.65	0.0276
Rnf11	Ring finger protein 11	-1.75	0.0244
Cntn1	Contactin 1	-1.79	0.0494
COXIII	Mitochondrial cytochrome oxidase II subunit	-1.83	0.0244
Ap3m2	Adapter-related protein complex 3, mu 2 subunit	-1.85	0.0231
Rnf11	Ring finger protein 11	-1.88	0.0060
Mif	Macrophage migration inhibitory factor	-1.91	0.0337
Pde1c	Phosphodiesterase 1C, calmodulin-depdendent 70kDa	-1.96	0.0053
Pcdha7	Protocadherin alpha 7	-1.98	0.0264
Extl3	Exostosin-like glycosyltransferase 3	-2.05	0.0291
Unc13a	Unc-13 homolog A	-2.11	0.0060
Gm5478	Predicted pseudogene 5478	-2.13	0.0103
Tmsb10	Thymosin beta 10	-2.15	0.0494
Pgk1	Phosphoglycerate kinase 1	-2.30	0.0414
Stmnd1	Stathmin domain containing 1	-2.42	0.0034
Mt2	Metallothionein 2	-2.50	0.0126
Yaf2	YY1 associated factor 2	-2.54	0.0473
Clip1	CAP-GLY domain containing linker protein 1	-2.75	0.0060
Slc7a3	Solute carrier family 7 (cationic amino acid transporter, Y+ system), 3	-2.87	0.0103
Abca1	ATP-binding cassette, sub-family A (ABC1), member 1	-3.10	0.0171
Them6	Thioesterase superfamily member 6	-3.24	0.0011
Hdac9	Histone deacetylase 9	-3.69	0.0029
Ptprr	Protein tyrosine phosphatase, receptor type, R	-3.72	0.0135
Naa11	N(alpha)-acetyltransferase 11, NatA catalytic subunit	-3.83	0.0004
Lynx1	Ly6/neurotoxin 1	-8.26	0.0135
Mt1	Metallothionein 1	-10.73	0.0015

Table S2. Differentially expressed genes in a microarray study comparing FACS-isolated EYFP-positive cells from degenerate and non-degenerate L7-Cre EYFP mouse retinas. Statistically significant, differentially expressed, probes are listed according to log fold change. A positive log fold change represents upregulation in the degenerate samples. "*p* value" represents the adjusted p-value following False Detection Rate (FDR) testing.

Probe	Log_2 fold Δ	p value
Receptor		
Grm6	1.054	0.8573
Gα subunits		
Gna11	1.04	0.7896
Gna11	-1.07	0.8574
Gna14	-1.08	0.7764
Gnai1	-1.09	0.9360
Gnai2	-1.04	0.8810
Gnai3	1.01	0.9863
Gnao1	-1.23	0.7900
Gnao1	1.02	0.9835
Gnaq	-1.40	0.0539
Gnaq	-1.03	0.8832
Gβγ subunits		
Gnb3	1.91	0.1685
Gnb4	-1.05	0.9335
Gnb5	-1.01	0.9670
Gng2	-1.10	0.8044
Gng3	1.34	0.8414
Gng5	1.04	0.8175
Gng7	1.64	0.6041
Gng7	1.07	0.7679
Gng10	-1.08	0.7839
Gng11	-1.05	0.8035
Gng13	-1.13	0.7109
Bipolar cell-specific		
Cabp5	1.48	0.5394
Pcp2	-1.12	0.8044
Prkca	-1.09	0.7514
Scgn	1.40	0.8044
Scgn	-1.02	0.9746
Vsx1	1.04	0.9102
Vsx2	1.21	0.8056
Vsx2	1.10	0.9021
Kinases		
Grk4	1.13	0.7241
Grk4	-1.07	0.7896
Grk5	1.09	0.7918
Grk5	1.04	0.8642

Probe	Log_2 fold Δ	p value
Intracellular effectors		
Adcy1	-2.97	0.0004
Adcy1	1.05	0.8044
Adcy2	1.77	0.5721
Adcy3	1.01	0.9480
Adcy8	1.06	0.8086
Adcy9	1.05	0.8035
Pde1b	-1.37	0.5764
Pde1b	-1.41	0.6178
Pde1c	-1.96	0.0053
Pde1c	-1.22	0.1861
Pde1c	-1.09	0.7629
Pde1c	1.19	0.7932
Pde1c	-1.10	0.8337
Pde1c	1.00	0.9986
Pde3a	-1.03	0.8542
Pde3a	1.01	0.9441
Pde3a	1.00	1.0000
Pde3b	-1.02	0.9259
Pde4a	-1.12	0.5721
Pde4b	-1.26	0.4073
Pde4b	-1.20	0.7671
Pde4b	1.27	0.8311
Pde4b	-1.02	0.9409
Pde4d	-2.05	0.5154
Pde4d	-1.00	0.9918
Pde7a	-1.06	0.7887
Pde7b	-1.16	0.6154
Pde8b	-1.02	0.8908
Pde9a	-1.55	0.0416
Plcb3	1.07	0.7536
Plcb4	1.24	0.8044
TRP channels		
Trpc6	-1.05	0.7749
Trpc7	-1.29	0.7887
Trpm1	1.19	0.7847
Trpm1	-1.13	0.8035
Trpm1	1.09	0.8220
Trpm1	1.19	0.8401
Arrestin		
Arrb2	-1.11	0.8673

Housekeeping genes					
Actb	1.45	0.6114	*Gapdh*	-1.51	0.1950
Actb	-1.31	0.7128	*Rplp0*	-1.15	0.8035
Actb	-1.03	0.9801	*Rplp0*	1.02	0.9900
Actb	-1.03	0.9802			

Table S3. In a microarray study comparing FACS-isolated EYFP-positive cells from degenerate and non-degenerate L7-Cre EYFP mouse retinas, genes related to intracellular communication, the native on-bipolar signal transduction cascade. A selection of "housekeeping" genes are included for comparison. A positive log fold change represents upregulation in degenerate samples. "p value" represents the adjusted p-value following False Detection Rate (FDR) testing. Note that multiple probes for some genes are reported in the above table, for clarity, all probes are labelled only with the associated gene name.

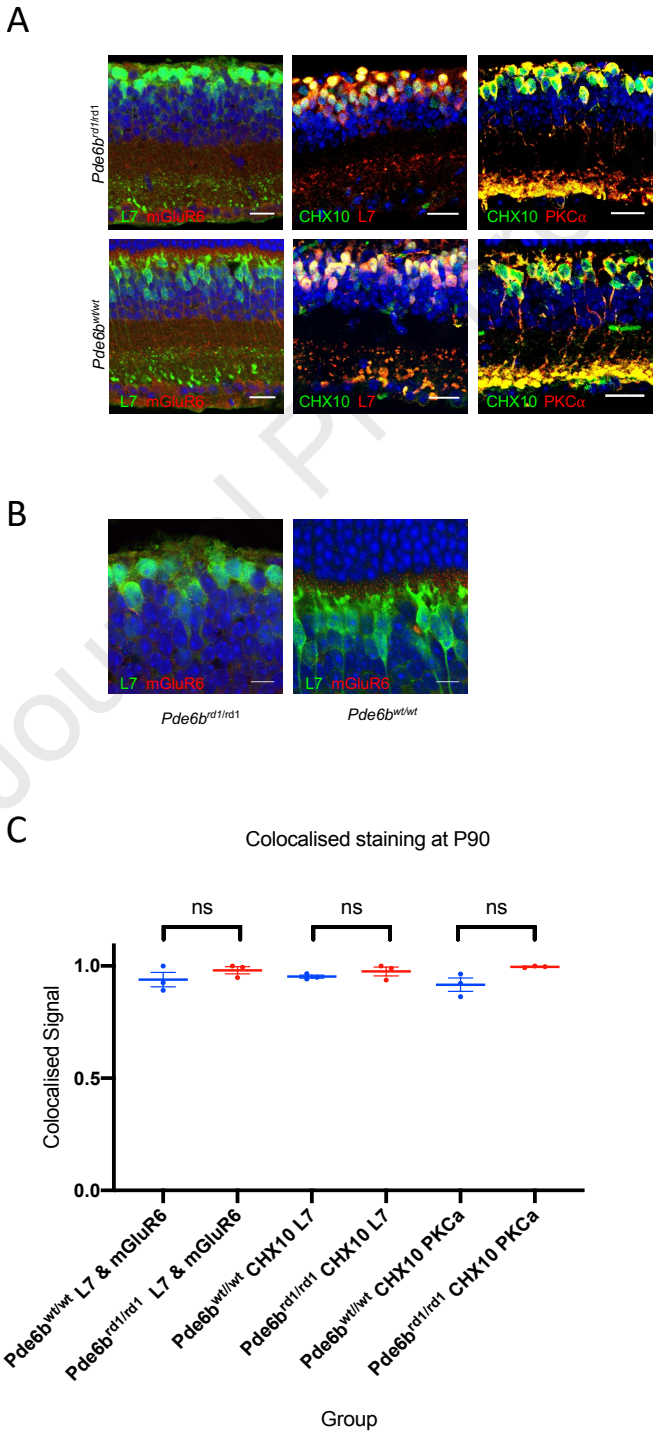
A
Pde6b rd1/rd1
L7 mGluR6
CHX10 L7
CHX10 PKCα
Pde6b wt/wt
L7 mGluR6
CHX10 L7
CHX10 PKCα
B
L7 mGluR6
L7 mGluR6
Pde6b rd1/rd1
Pde6b wt/wt
C
Colocalised staining at P90
ns
ns
ns
1.0
0.5
0.0
Colocalised Signal
Pde6b wt/wt L7 & mGluR6
Pde6b rd1/rd1 L7 & mGluR6
Pde6b wt/wt CHX10 L7
Pde6b rd1/rd1 CHX10 L7
Pde6b wt/wt CHX10 PKCa
Pde6b rd1/rd1 CHX10 PKCa
Group

(Fig S3.)

Figure S3.

A. Immunohistochemical staining of retina from *Pde6b*$^{rd1/rd1}$ and *Pde6b*$^{wt/wt}$ mice culled at P90 for proteins associated with the bipolar signalling cascade (mGluR6, PKCα & L7 – none of which demonstrated significant changes in gene expression between *Pde6b*$^{rd1/rd1}$ and *Pde6b*$^{wt/wt}$ - see table S3). In all panels, DAPI staining is in blue, other colours as indicated in panels scale bar = 20μm main panels.
B. Higher magnification views of mGluR6 staining in the outer plexiform layer . Note particularly the punctate pattern of staining of the bipolar cells dendrites in the wild type. Note L7 staining covers cell bodies and dendrites. Scale bars =10μm.
C. Colocalised pixels above threshold - a semiquantitative index of protein expression based on immunohistochemical staining. Normalised to highest value over all retinae stained for the same proteins. t-tests did not reveal a difference in mean values between *Pde6b*$^{rd1/rd1}$ and *Pde6b*$^{wt/wt}$ retinae stained for the same proteins ($p>0.05$). NS = not-significant.

Probe	Log_2 fold Δ	p value
Kainate type		
Grik1	1.57	0.6786
Grik1	1.07	0.7896
Grik1	1.13	0.7934
Grik1	1.09	0.8785
Grik1	-1.03	0.9705
Grik4	-1.01	0.9784
Vglut transporter		
Slc17a6	-1.05	0.8679
Slc17a6	-1.01	0.9865
Slc17a7	-1.05	0.8592
Slc17a8	-1.08	0.7415

Probe	Log_2 fold Δ	p value
AMPA type		
Gria1	-1.39	0.7587
Gria1	1.05	0.8440
Gria1	1.04	0.8681
Gria1	1.04	0.8708
Gria2	1.27	0.6526
Gria2	1.21	0.7415
Gria3	-1.04	0.8035
Gria3	-1.06	0.9259
Gria4	1.07	0.7587
NMDA type		
Grin2c	-1.02	0.9094

GABA and Glycine receptor subunits

GABA		
Gabra1	-1.05	0.8824
Gabra3	1.07	0.8194
Gabrb1	1.01	0.9632
Gabrb2	1.11	0.6142
Gabrb2	1.01	0.9870
Gabrb3	1.12	0.7500
Gabrb3	-1.11	0.8013
Gabrb3	-1.03	0.9382
Gabrg2	-1.56	0.0494
Gabrg2	-1.48	0.6302
Gabrg2	-1.36	0.6308
Gabrg2	1.06	0.7420
Gabrg2	-1.06	0.8721
Gabrg2	-1.10	0.9477
Gabrr1	-1.56	0.5706
Gabrr1	-1.04	0.8718
Gabrr2	-1.16	0.7896

Glycine		
Glra2	-1.06	0.8015
Glra4	1.09	0.7753
Glrb	1.07	0.7969

Table S4. In a microarray study comparing FACS-isolated EYFP-positive cells from degenerate and non-degenerate L7-Cre EYFP mouse retinas, genes relating to glutamate, glycine and gaba receptors;. A positive log fold change represents upregulation in degenerate samples. “P value” represents the adjusted p-value following False Detection Rate (FDR) testing. Note that multiple probes for some genes are reported in the above table, for clarity, all probes are labelled only with the associated gene name.

Protein of Interest	Antibody (source & product number)	Plasmid used in validation ICC
ANNEXINa7	Abcam ab197586	Source bioscience plasmid no. 3157926
CONTACTIN1	Abcam ab66265	Sino biologic plasmid no. MG50933
SHROOM2	Atlas hpa051646	GenScript plasmid no. OMu14281D
SULPHATASE2	Abcam ab113405	Addgene plasmid no. 13008
CHX10	Abcam ab16141	See Kim et al [REFERENCE Kim et al 2008]
PKCα	Abcam ab32376	See Ruether et al [REFERENCE Ruether et al 2010]

(Table S5)

Table S5. Antibodies and plasmids used in their validation

—

MJ Gilhooley, D Hickey, M Lindner, T Palumaa, S Hughes, S Peirson, RE MacLaren, MW Hankins

"ON-bipolar cell gene expression during retinal degeneration: implications for optogenetic visual restoration"

Figures & Tables

February 2021

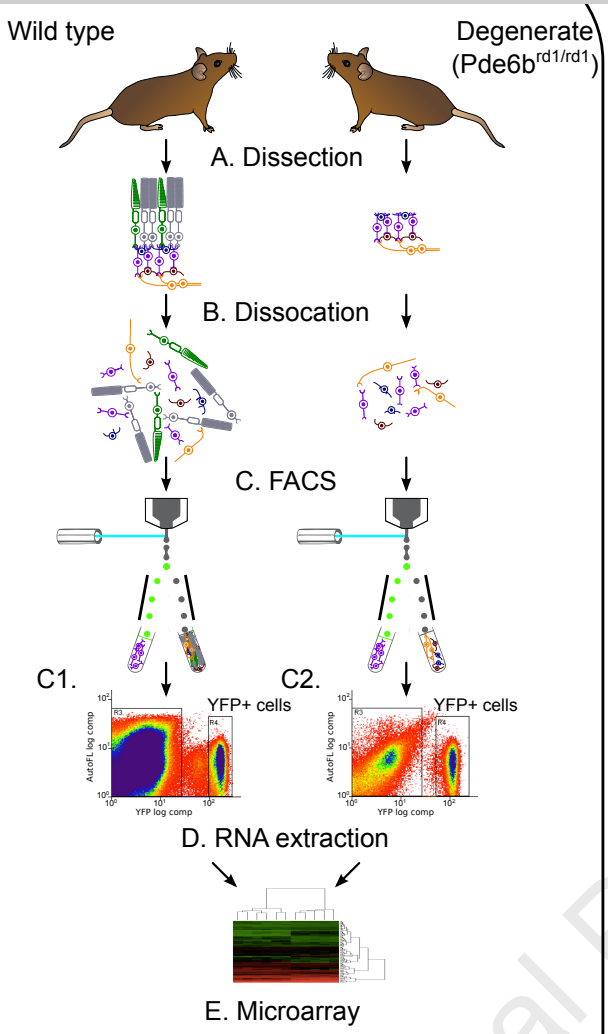

1.1 Experimental Approach

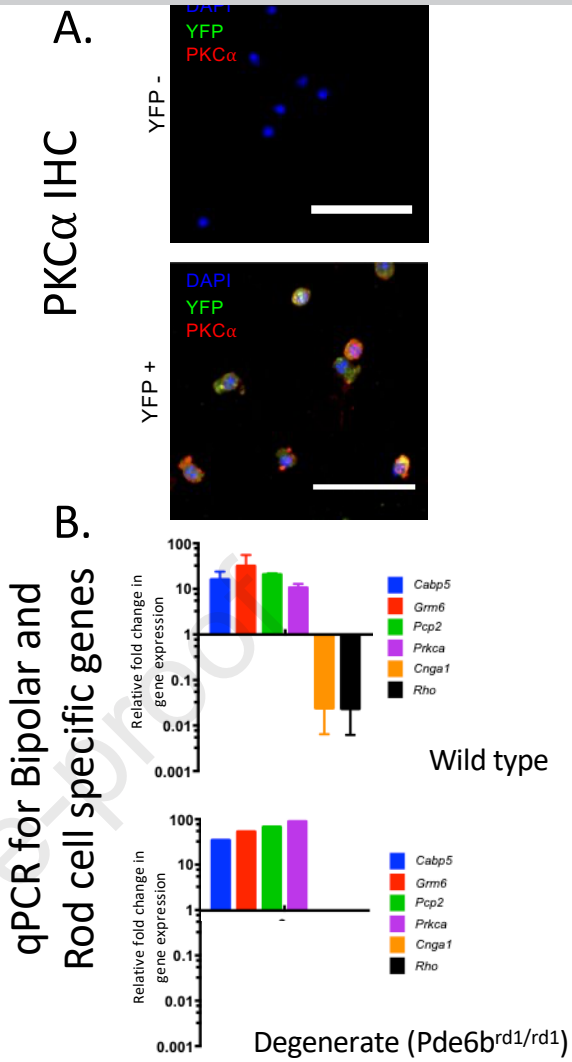

1.2 FACS Validation

Figure 1.

1.1 Experimental Approach: fluorescence-activated cell sorting for a microarray study of retinal bipolar cells from degenerate retinas. (A)L7-Cre EYFP non-degenerate (*Pde6bwt/wt*) and degenerate (*Pde6brd1/rd1*) mice were culled at P90 and the retinae removed with careful dissection to remove Retinal Pigment Epithelium before dissociation (B) FACS was then used to isolate YFP-positive (ON-Bipolar) cells (C). From this isolate, RNA was extracted (D) and used for a microarray study. Panel (C1) represents an illustrative FACS dot plot of a single dissociated, non-degenerate L7.Cre.EYFP retinae and (C3) the same from a degenerate retina.

1.2 FACS Validation. Methods to confirm the identity of isolated YFP+ cells. (A) Immunocytochemistry (ICC) of YFP positive and YFP negative FACS isolate from wildtype retina stained for DAPI (blue), PKCa (red) and YFP (green) showing, as expected enrichment of PKCα + (bipolar) cells in the YFP+ isolate. Scale bars = 50µm. (B) Quantitative PCR (qPCR) comparing expression of retinal bipolar cell-specific and rod cell-specific genes in the YFP-positive cell population, relative to the YFP- negative cell population in samples from a small number of wildtype and degenerate ($Pde6b^{rd1/rd1}$) L7-Cre EYFP retinas following FACS at P90. The YFP-positive cell fraction had higher expression of bipolar-specific and lower expression of rod-specific genes, indicating that the YFP-positive population was enriched in bipolar cells (mean ± s.e.m.; n = 2, non- degenerate, n = 1, degenerate).

Symbol	Δ $\log_2$	Ontology term 1	Ontology term 2
A - Actin cytoskeleton, microtubules and intracellular transport			
Ap3m2	-1.85	anterograde synaptic vesicle transport	intracellular protein transport
Cng	3.52	microtubule cytoskeleton organization	microtubule binding
Sept4	1.54	cilium assembly	mitotic cytokinesis
Srm2	**1.81**	**actin cytoskeleton organization**	**melanosome organization**
Tmsb1	-2.15	actin cytoskeleton organization	regulation of cell migration
B - Heparin sulphate proteoglycan metabolism			
Extl3	-2.05	heparan sulphate proteoglycan biosynthesis	protein glycosylation
Sulf2	**1.43**	**heparan sulphate proteoglycan metabolic process**	**arylsulfatase activity**
C - Cell signalling, calcium homeostasis			
Anxa7	**-1.56**	**calcium ion binding**	**membrane fusion**
Cabyr	2.25	sperm capacitation	calcium-mediated signalling
Gabrg2	-1.56	gamma-aminobutyric acid signalling pathway	synaptic transmission, GABAergic
Pde1c	-1.96	signal transduction	response to calcium ion
Slc7a3	-2.87	amino acid transport	arginine transport
Unc13a	-2.11	neurotransmitter secretion	SNARE binding
D - Neural cell growth, survival & remodeling			
Cntn1	**-1.79**	**neuron projection development**	**nervous system development**
Efnb1	2.15	axon guidance	presynapse assembly
Hdac9	-3.69	DNA repair	chromatin organization
Lynx1	-8.26	synaptic transmission, cholinergic	acetylcholine receptor binding
Mif	-1.91	regulation of cell proliferation	positive regulation of axon regeneration
Nrm	-1.40	nuclear membrane	membrane
Pcdha7	-1.98	cell adhesion	cell-cell recognition
Phc1	1.93	cellular response to retinoic acid	histone ubiquitination
Ptprr	-3.72	negative regulation of ERK1 and ERK2 cascade	ERBB2 signalling pathway
Sfrs1	1.72	mRNA 5'-splice site recognition	regulation of transcription, DNA-templated
Socs5	-1.64	regulation of growth	JAK-STAT cascade
Yaf2	-2.54	regulation of transcription, DNA-templated	transcription, DNA-templated
E - Aerobic and anaerobic respiration, cellular response to stress			
Atox1	-1.62	transition metal ion binding	response to oxidative stress
Clip1	-2.75	transition metal ion binding	microtubule bundle formation
Cox3	-1.83	aerobic electron transport chain	aerobic respiration
Msrb2	3.03	transition metal ion binding	cellular response to stress
Mt1	-10.73	transition metal ion binding	cellular metal ion homeostasis
Ndufb2	-1.55	mitochondrial respiratory chain complex I	oxidation-reduction process
Pgk1	-2.30	glycolytic process	carbohydrate metabolic process
F - Miscellaneous			
Abca1	-3.10	cholesterol homeostasis	cellular response to retinoic acid
Fam19a3	1.87	positive regulation of microglial cell activation	negative regulation of microglial cell activation
Naa11	-3.83	n-terminal protein amino acid acetylation	n-terminal peptidyl-glutamic acid acetylation
Rnf11	-1.75	protein autoubiquitination	ubiquitin-dependent protein catabolic process

Table 1. Genes differentially expressed between *Pde6b*$^{rd1/rd1}$ and *Pde6b*$^{+/+}$ retinae at P90, grouped by broad function based on gene ontology terms annotated to the gene's entry on the gene ontology consortium database (two listed for each gene). Δ = change in expression compared to *Pde6b*$^{wt/wt}$ (ie. '+' = up regulated; '-' = down regulated) please see table S2 for corresponding FDR adjusted p-values.

Gene	*Srm2*	*Sulf2*	*Anxa7*	*Cntn1*
Protein	Shroom 2	Sulphatase 2	Annexin a7	Contactin 1
Function	Actin cytoskeleton, axon guidance	HSPG metabolism	Membrane fusion, neurotransmitter release	Neuron projection development, synaptic remodelling
Comments	Regulates actin cyctoskeleton and therefore cell shape, axon sprouting and organelle location (essential for viral transduction, second messenger systems and neurotransmitter release) (Fairbank et al., 2006).	Extracellular endosulphatase. Removes sulphate residues from cell surface HSPG residues(Morimoto-Tomita et al., 2002) - important in the entry of AAV into cells(Summerford and Samulski, 1998) as well as retinal synaptic plasticity	Calcium dependant phospholipid binding protein implicated in synaptic neurotransmitter release and the bipolar cell light response(Caohuy and Pollard, 2002; Grewal et al., 2016; Hoque et al., 2014). PKCα (important in activation and termination of bipolar cell light response phosphorylates annexin a7 promoting membrane fusion and so neurotransmitter release(Hoque et al., 2014). PKCα expression was not altered in our gene array comparison.	A cell surface glycoprotein implicated in synaptic plasticity(Davisson et al., 2011)
Human disease caused defect in gene	Implicated in retinal degeneration with deafness(Fairbank et al., 2006)	Not reported	Not reported	Congenital Myopathy(Davisson et al., 2011)
Mouse knock outs	Knock down - failure of retinal lamination, full knock out - no retinal phenotype. Other S*rm* family members may compensate. (Fairbank et al., 2006)	Deficiencies in neural remodelling; no major developmental flaws or retinal defects reported(Masu, 2013)	No gross neurological phenotype, retina not examined(Grewal et al., 2016)	Impaired synaptic long-term depression (LTD)(Murai et al., 2002). Over-expression improves long term potentiation (LTP)(Gulisano et al., 2017). No retinal phenotype at P14(Chatterjee et al., 2019)
Expression at P90 (gene array)in $Pde6b^{rd1/rd1}$vs $Pde6b^{wt/wt}$ (FDR adj' p value)	Up (p=0.042)	Up (p=0.034)	Down (p=0.024)	Down (p=0.049)
Expected location of protein within cell	Cell membrane(Etournay et al., 2007) confirmed in cell culture (*figure S1*) & IHC (*figure 2*)	Cell surface, extracelluar(Morimoto-Tomita et al., 2002) Confirmed in cell culture (*figure S1*) & IHC (*figure 3*)	Cell membrane(Watson et al., 2004) confirmed in cell culture (*figure S1*) & IHC (*figure 4*)	Cell surface(Davisson et al., 2011), confirmed in cell culture (*figure S1*) & IHC (*figure 5*)
Previous IHC of $Pde6b^{wt/wt}$ retinae	Retinal pigment epithelium, bipolar cell bodies, inner plexiform layer(Etournay et al., 2007)	Bipolar cell bodies, outer plexiform layer photoreceptors synapses(Orlandi et al., 2018)	Not described previously in retina	Bipolar cell and outer plexiform layer(Davisson et al., 2011)
2-way ANOVA – difference by genotype ($Pde6b^{rd1/rd1}$vs $Pde6b^{wt/wt}$)	Yes F(1, 8) = 23.85; p=0.0012	No F(1, 8) = 3.775; p=0.0879	Yes F(1, 9) = 5.31; p=0.0467	Yes F(1, 13) = 8.272; p=0.0130
2-way ANOVA – difference by time	Yes F(3, 8) = 4.865; p=0.0327	Yes F(3,8) = 19.9; p=0.005	No F(3, 9) = 0.1829; p=0.9053	No F(3, 13) = 0.168; p=0.9161
2-way ANOVA - interaction genotype x time	Yes F(3,8) = 9.09; p=0.0059	No F(3,8) = 2.718; p=0.1148	No F(3,9) = 0.6712; p=0.5909	Yes F(3,13) = 7.366; p=0.0039
Significant Post Hoc Tests	Sidak P90 – p=0.0136; p120 - p=0.0026 Tukey $Pde6b^{rd1/rd1}$:P40 vs P150 p=0.0307; P90 vs P150 p=0.0157; $Pde6b^{wt/wt}$:P40 vs P120 p=0.0126); P120 vs P150 p= 0.0199	Tukey $Pde6b^{rd1/rd1}$:P40v s P90 p=0.0083; P90 vs P150 p=0.0028; P120 to P150 p=0.0248; $Pde6b^{wt/wt}$: P40 vs P150 p=0.0146; P90 vs P150 p=0.0052; P120 vs P150 p=0.0116	Sidak Not significant at any individual timepoint	Sidak P90 p=0.0026

Table 2 Details of four differentially expressed genes prioritised for further characterisation with IHC. The bottom four rows refer to semiquantitative IHC co-localisation seen in figure 2,3,4 and 5. *p*= - “adjusted p value”; n.s. – P>0.05

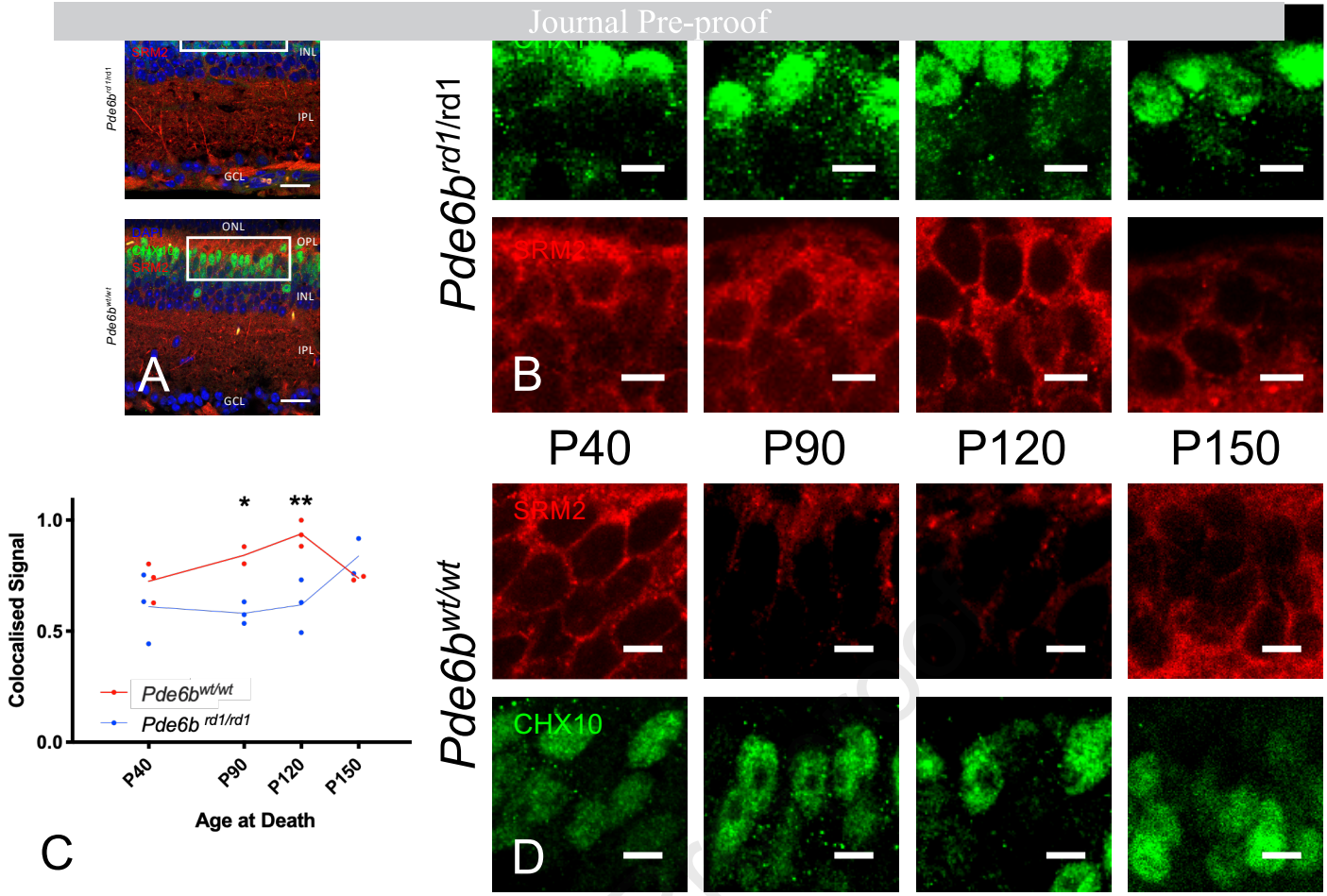

Figure 2. Shroom 2 immunohistochemistry

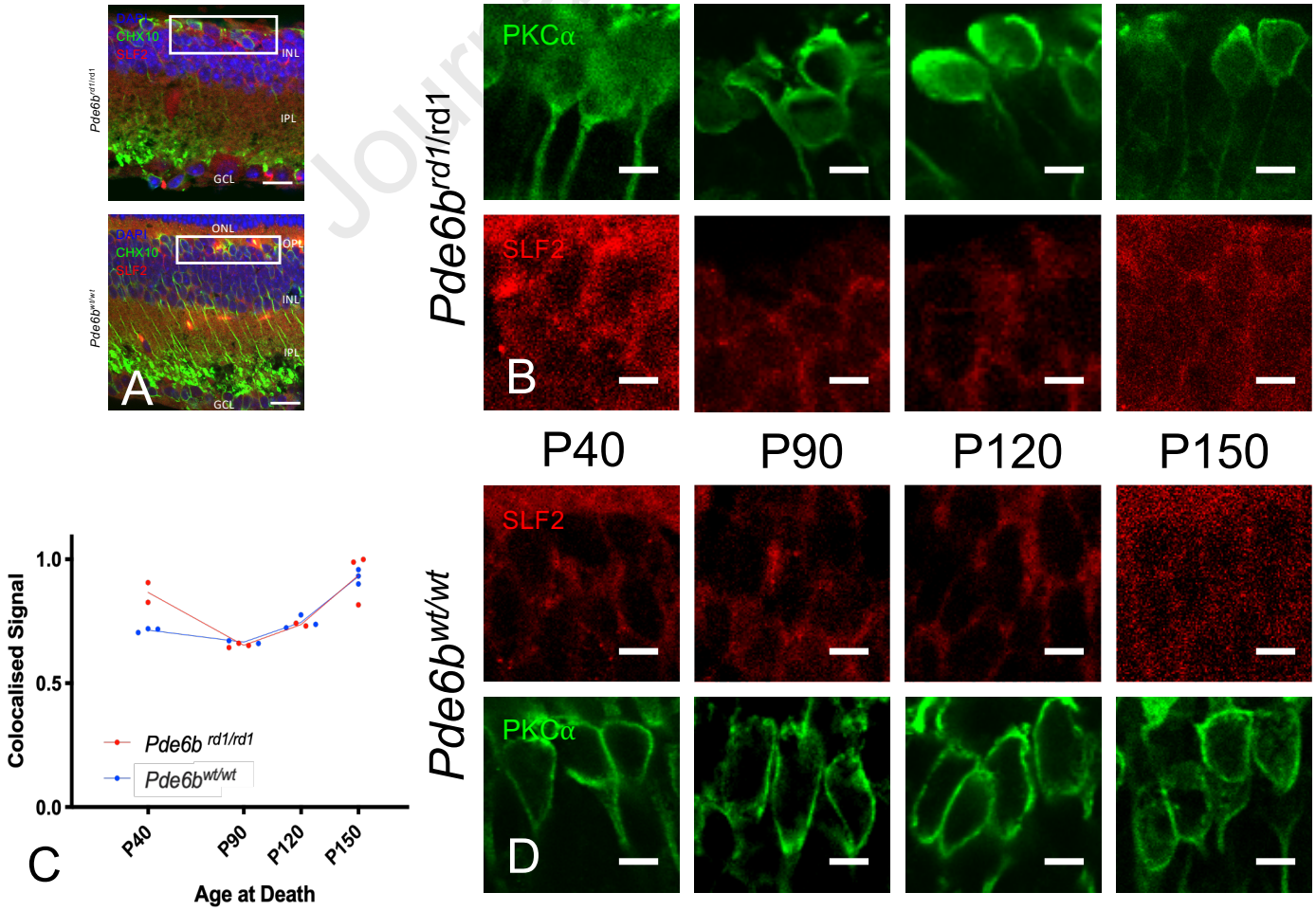

Figure 3. Sulphatase 2 immunohistochemistry

Figure 2. Shroom 2 Immunohistochemistry (upregulated on gene array at P90)

(A) Retinal cross sections from Pde6b$^{rd1/rd1}$ and Pde6b$^{wt/wt}$ mice stained for DAPI (blue), CHX10 (green) and Shroom2 (red). ONL – Outer nuclear layer, OPL – Outer Plexiform layer, INL- Inner nuclear layer, IPL –inner plexiform layer, GCL – Ganglion cell layer. Scale bar = 20µm. White box indicates area from which close up images in panels B & D are taken.

(B&D) Close up images of bipolar cell bodies in *Pde6b$^{rd1/rd1}$* retina (B) and *Pde6b$^{wt/wt}$* (D) at four time points during degeneration (P40, P90, P120, P150). CHX10 (green) and shroom 2 (red). Scale bars = 5µm

(C) Colocalised pixels above threshold - a semiquantitative index of protein expression. Normalised to highest value over all retinae stained for shroom 2. Dots represent the mean value for each animal, lines connect the means for each group at that timepoint. Star markers on graph represent adjusted p values, Sidak's method for multiple comparison (see results section for details): P90 p=0.0136; P120 p=0.0026 red line = *Pde6b$^{rd1/rd1}$*; blue line = *Pde6b$^{wt/wt}$.*

Figure 3. Sulphatase 2 Immunohistochemistry (upregulated on gene array at P90)

(A) Retinal cross sections from Pde6b$^{rd1/rd1}$ and Pde6b$^{wt/wt}$ mice stained for DAPI (blue), PKCα (green) and sulphtase 2 (red). ONL – Outer nuclear layer, OPL – Outer Plexiform layer, INL- Inner nuclear layer, IPL –inner plexiform layer, GCL – Ganglion cell layer. N.B. Due to primary antibodies being raised in differing species, to allow co-staining of sections, PKCα is used as an ON-bipolar marker here, rather than CHX10. Scale bar = 20µm. White box indicates area from which close up images in panels B & D are taken.

(B&D) Close up images of bipolar cell bodies in *Pde6b$^{rd1/rd1}$* retina (B) and *Pde6b$^{wt/wt}$* (D) at four time points during degeneration (P40, P90, P120, P150). PKCα (green) and Sulphatase 2 (red). Scale bars = 5µm

(C) Colocalised pixels above threshold - a semiquantitative index of protein expression. Normalised to highest value over all retinae stained for Sulphatase 2. Dots represent the mean value for each animal, lines connect the means for each group at that timepoint. Star markers on graph represent adjusted p values, Sidak's method for multiple comparison (ie. None reaching significance, see results section for details). red line = *Pde6b$^{rd1/rd1}$*; blue line = *Pde6b$^{wt/wt}$*

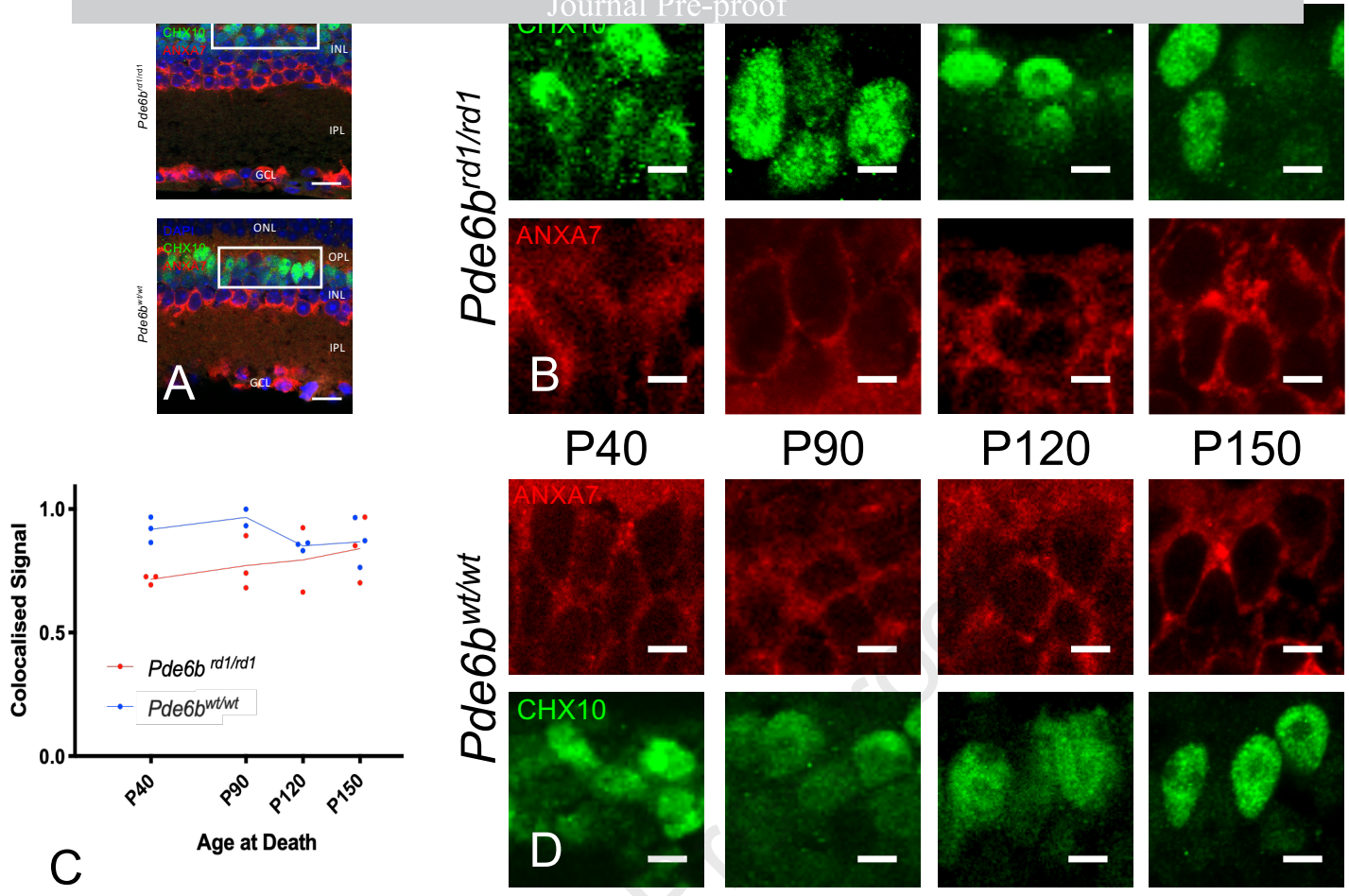

Figure 4. Annexin a7 immunohistochemistry

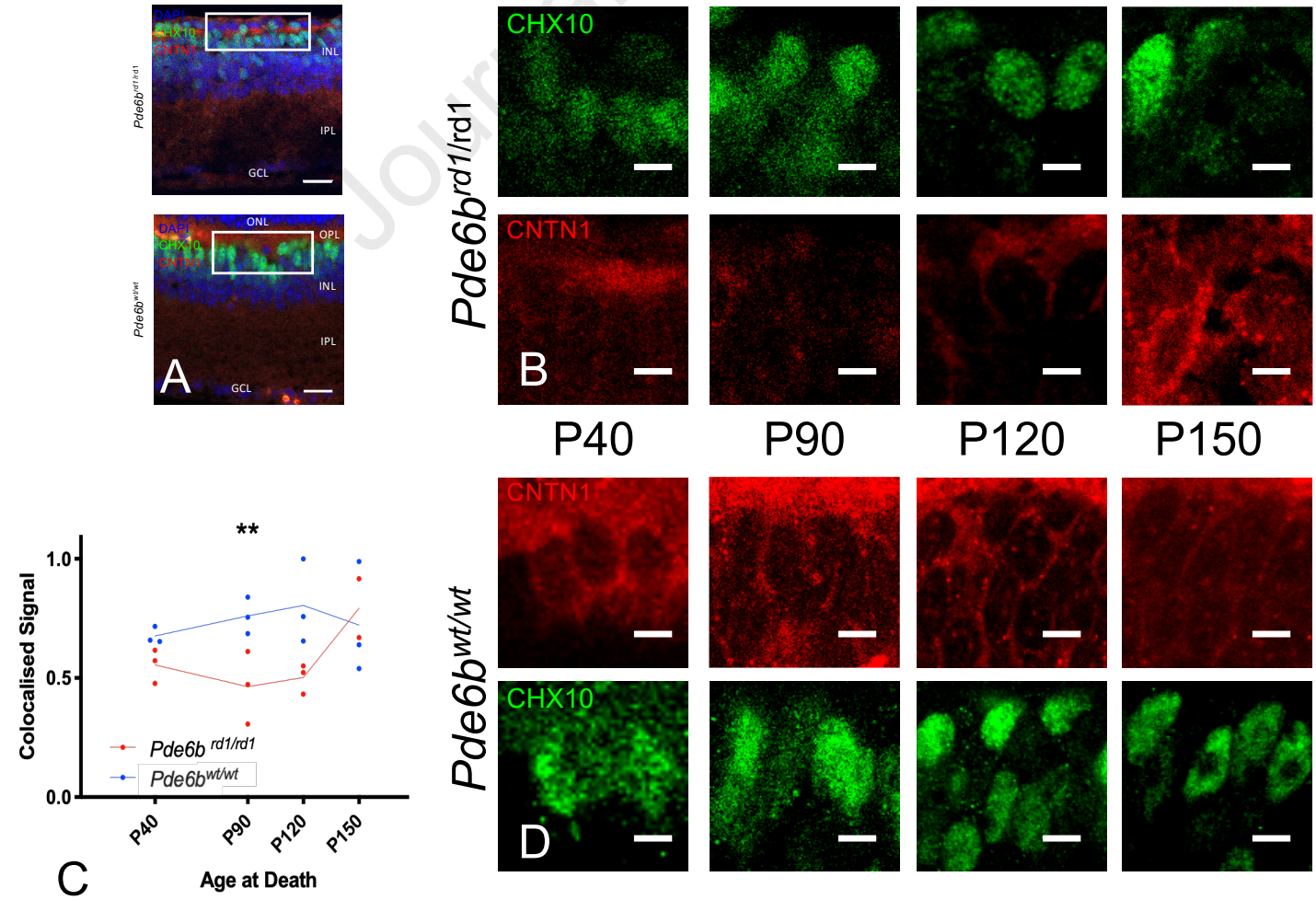

Figure 5. Contactin 1 immunohistochemistry

Figure 4. Annexin a7 Immunohistochemistry (downregulated on gene array at P90).

(A) Retinal cross sections from Pde6b$^{rd1/rd1}$ and Pde6b$^{wt/wt}$ mice stained for DAPI (blue), CHX10 (green) and annexin a7 (red). ONL – Outer nuclear layer, OPL – Outer Plexiform layer, INL- Inner nuclear layer, IPL –inner plexiform layer, GCL – Ganglion cell layer. Scale bar = 20µm. White box indicates area from which close up images in panels B & D are taken.

(B&D) Close up images of bipolar cell bodies in *Pde6b$^{rd1/rd1}$* retinae (B) and *Pde6b$^{wt/wt}$* (D) at four time points during degeneration (P40, P90, P120, P150). CHX10 (green) and annexin a7 (red). Scale bars = 5µm.

(C) Colocalised pixels above threshold - a semiquantitative index of protein staining. Normalised to highest value over all retinae stained for annexin a7. Dots represent the mean value for each animal, lines connect the means for each group at that timepoint. Star markers on graph represent adjusted p values, Sidak's method for multiple comparison (ie. None reaching significance, see results section for details). red line = *Pde6b$^{rd1/rd1}$*; blue line = *Pde6b$^{wt/wt}$*

Figure 5. Contactin1 Immunohistochemistry (downregulated on gene array at P90).

(A) Retinal cross sections from Pde6b$^{rd1/rd1}$ and Pde6b$^{wt/wt}$ stained for DAPI (blue), CHX10 (green) and Contactin 1 (red). ONL – Outer nuclear layer, OPL – Outer Plexiform layer, INL- Inner nuclear layer, IPL – inner plexiform layer, GCL – Ganglion cell layer. Scale bar = 20µm. White box indicates area from which close up images in panels B & D are taken.

(B&D) Close up images of bipolar cell bodies in *Pde6b$^{rd1/rd1}$* retina (B) and *Pde6b$^{wt/wt}$* (D) at four time points during degeneration (P40, P90, P120, P150). CHX10 (green) and Contactin 1 (red). Scale bars = 5µm.

(C) Colocalised pixels above threshold - a semiquantitative index of protein expression. Normalised to highest value over all retinae stained for Contactin 1. Dots represent the mean value for each animal, lines connect the means for each group at that timepoint. Star markers on graph represent adjusted p values, Sidak's method for multiple comparison at P90 p=0.0026) (see results section for details). red line = Pde6b$^{rd1/rd1}$; blue line = *Pde6b$^{wt/wt}$*

Highlights

- Bipolar cells are attractive targets for therapeutic optogenetics in IRDs
- This is the first cell specific transcriptomic analysis of bipolar cells in an IRD model
- Bipolar cells maintain expression of genes essential to act as targets for optogenetics
- Protein staining relating to four candidate genes (*Anxa7, Cntn1, Srm2, Sulf2*) is confirmed using immunohistochemistry